[2] W. J. Evans and G. I. Haddad, "Frequency conversion in IMPATT diodes," *IEEE Trans. on Electron Devices*, vol. ED-16, pp. 78–87, Jan. 1969.
[3] M. E. Hines, "Large signal noise, frequency conversion, and parametric instabilities in IMPATT diode networks," *Proc. IEEE*, vol. 60, pp. 1534–1548, Dec. 1972.
[4] W. E. Schroeder and G. I. Haddad, "Effects of harmonic and subharmonic signals on avalanche-diode oscillator performance," *IEEE Trans. M.T.T.*, vol. MTT-18, pp. 327–331, June 1970.
[5] G. Salmer, E. Allamando, E. Constant, and A. Semichon, "Frequency multiplication using an avalanche diode," presented at the M.O.G.A. Conference, Amsterdam, The Netherlands, 1970.
[6] P. A. Rolland, G. Salmer, M. Chive, and J. Michel, "High rank frequency multiplication using avalanche diode," in *Proc. Fourth Biennial Cornell Conf.*, Cornell University, Ithaca, NY, 1973.
[7] P. A. Rolland, G. Salmer, A. Derycke, and J. Michel, "Very high rank avalanche diode frequency multiplier," *Proc. IEEE*, vol. 61, pp. 1757–1758, 1973.
[8] P. A. Rolland, E. Constant, A. Derycke, and J. Michel, "Multiplication de fréquence par diode à avalanche en ondes millimétriques," *Acta Electronica*, vol. 17, pp. 213–228, Apr. 1974.
[9] P. A. Rolland, Third cycle thesis (Lille I University, France, 1973).
[10] P. L. Ntake and D. R. Conn, "Frequency multiplication by a PIN diode when driven into avalanche breakdown," *IEEE Trans. M.T.T.*, vol. MTT-23, pp. 477–485, June 1975.
[11] J. L. Vaterkowski, E. Constant, and Y. Druelle, "A *Ka* band up converter using avalanche diodes," in *Proc. 4th Eur. Microw. Conf.*, Montreux, Switzerland, Sept. 1974.
[12] G. Salmer, J. Pribetich, A. Farrayre, and B. Kramer, "Theoretical and experimental study of GaAs IMPATT oscillator efficiency," *J. Appl. Phys.*, vol. 44, pp. 314–324, 1973.
[13] E. Allamando, thesis (Lille I University, France, 1973).
[14] B. B. van Iperen and H. T. Tjassens, "Influence of carrier velocity saturation in the unswept layer on the efficiency of avalanche transit time diodes," *Proc. IEEE*, vol. 59, pp. 1032–1033, 1971.
[15] C. A. Lee, R. L. Batdorf, W. Wiegmann, and G. Kaminsky, *J. Appl. Phys.*, vol. 38, p. 2787, 1967.
[16] W. J. Evans, "Computer experiments on TRAPATT devices," *IEEE Trans. M.T.T.*, vol. MTT-18, pp. 862–871, Nov. 1970.
[17] Y. Fukatsu, and H. Kato, "Frequency conversion with gain through sideband locking of an IMPATT diode oscillator," *Proc. IEEE*, vol. 57, pp. 342–343, Mar. 1969.
[18] P. A. Rolland, thesis to be published.
[19] J. L. Vaterkowski, thesis to be published.
[20] M. Gilden and M. E. Hines, *IEEE Trans. Electron. Devices*, vol. ED-13, p. 169, 1966.

InP Gunn-Effect Devices for Millimeter-Wave Amplifiers and Oscillators

ROBERT J. HAMILTON, JR., MEMBER, IEEE, ROBERT D. FAIRMAN, MEMBER, IEEE, STEPHEN I. LONG, MEMBER, IEEE, MASAHIRO OMORI, AND F. BERINGER FANK

***Abstract*—CW InP Gunn oscillator performance has been extended up in frequency to the 26.5–40 and 50–75-GHz ranges. CW power outputs of 78 mW at 56 GHz have been attained to date. Amplifier evaluation in *Ka* band yielded useful gain from 26.5 to 40 GHz in two half-band circuits with noise figures ranging from 12.4 to 16.5 dB on flat profile devices. In a narrow-band amplifier circuit at 23 GHz, a device noise figure of 10.1 dB was obtained at 9-dB gain. A description of material growth, evaluation techniques, and device designs is also presented.**

I. Introduction

INTEREST in InP for transferred-electron oscillators and amplifiers has been increasing recently owing to its potential for high efficiency and low noise. Experimental results have been reported which confirm these attractive characteristics. Peak output powers of 8.5 W at 18-percent efficiency and 5 W at 24-percent efficiency have been reported under low-duty-cycle pulsed operation in *Ku* band [1]. Although the thermal conductivity of InP is higher than GaAs, because of InP's high threshold field (10 kV/cm) power densities are high and efficient CW operation is limited to 18 GHz and above (except for very low *nl* product amplifier devices) by thermal restraints. Under CW operation, efficiencies up to 10 percent at 22 GHz and 6 percent at 27 GHz have also been achieved [2], [24]. CW narrow-band reflection amplifiers have provided noise figures as low as 7.5 dB at 33 GHz [3] and 10.7 dB at 14 GHz [4], while theoretical predictions of 4 dB for optimum cathode notch structures have been published [5].

The investigations reported in this paper are being directed toward development of high-efficiency InP sources and wide-band low-noise amplifiers above 26 GHz. In order to accomplish this, vapor-phase InP epitaxial growth reactors have been optimized for control of the thin layers required for high-frequency operation. Material characterization methods have been designed for increased measurement accuracy on InP so that layers can be evaluated for carrier concentrations and impurity levels over a wide range of doping. Device fabrication methods, originally utilized on GaAs devices, have been adapted for InP requirements.

II. Device Technology

The application of InP for CW transferred-electron oscillators and amplifiers in the millimeter-wave range provides significant performance improvements over the more widely utilized GaAs devices. In particular, InP is a

Manuscript received February 16, 1976; revised May 10, 1976. This work was performed in conjunction with contracts for millimeter-wave InP device development from the Naval Electronics Laboratory Center, San Diego, CA, and U.S. Army Electronics Command, Fort Monmouth, NJ.

The authors are with the Solid State West Division, Varian Associates, Palo Alto, CA 94303.

superior material in several respects. It has a current peak-to-valley ratio of 3.5 as opposed to 2.5 for GaAs [2]. This, in theory, will provide higher oscillator conversion efficiencies. In addition, the peak-to-valley ratio degrades less rapidly with temperature changes than GaAs and the thermal conductivity is greater, thus favoring CW operation [6]. Due to the high effective transit velocity (1.3×10^7 cm/s) and fast intervalley scattering [7], longer active regions and higher ultimate frequency limitations should favor InP for millimeter-wave applications. Finally, InP reflection amplifiers have demonstrated extremely low noise figures (as low as 7.5 dB) [3], which have been attributed to the lower ratio of electron diffusion to mobility in this material [8].

Another important characteristic of InP is its higher threshold field. Because the threshold field is three times that of GaAs, power densities are much higher. Therefore, thermal limitations under CW operation are more significant, limiting practical CW devices to operation above 18 GHz (where active region lengths are short enough to permit effective heat transfer) or to bias polarities in which the anode is located at the heat sink. Because of the higher electric fields and more critical thermal interactions, CW InP devices are more dependent on bias voltage and current levels than equivalent GaAs devices.

In this effort, InP epitaxial one- and two-layer structures have been grown for operation as Gunn oscillators and amplifiers in the 18–26.5, 26.5–40, and 50–75-GHz frequency ranges with active layer thicknesses from 2 to 5 μm. These layers were grown by the PCl_3, In, H_2 vapor-phase (VPE) process [9] on high-quality InP substrates doped with either chromium or tin. The substrates were grown in this laboratory by the liquid encapsulated Czochralski technique.

Many of the techniques used to control impurity profiles in GaAs growth have been used successfully in maintaining flat, uniformly doped profiles in VPE InP [10], [11]. Device active layers require net carrier concentrations in the range of 1×10^{15}–1×10^{16} cm^{-3}. This has been accomplished both by control of PCl_3 mole fraction [12] and by vapor doping with H_2S. The PCl_3 control affects the equilibriums between the reactants and the donor impurities present, and is influenced directly by small differences in material purity in the quartz, PCl_3, or In.

Vapor doping with H_2S has been used for control of doping profiles, buffer layers, and contact layers. Buffer layers have been found to be essential in eliminating high-resistivity interface layers between the substrate and active region. This intentional sulfur back doping can be used to produce layer doping much more independent of background effects. A comparison of the two methods is shown in Fig. 1.

The InP layers grown were evaluated by capacitance–voltage (C–V), Van der Pauw, and photoluminescence (PL) measurements. The carrier concentration profile is obtained from the C–V data, the mobility and the carrier concentration from the Van der Pauw measurement, and the impurity levels from the PL measurement. Because of the low barrier

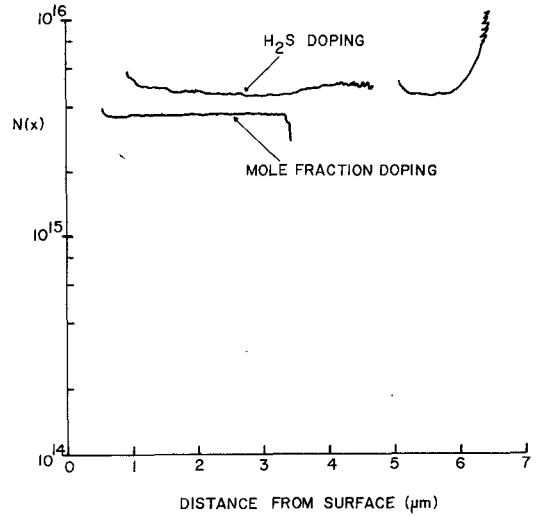

Fig. 1. Typical doping profiles for n-type InP layers. Sulfur doping and mole-fraction doping control are compared.

height for the metal-to-InP Schottky-barrier junction, no successful technique for reverse-bias capacitance measurement at room temperature has been reported. One way to circumvent this problem is to use a metal–insulator–semiconductor structure [13] instead of a metal–semiconductor junction. However, for the millimeter-wave application, the required device thickness is small, and growing and removal of a thin oxide layer on the semiconductor is time consuming and undesirable. Instead, the Au–InP Schottky-barrier system was used to obtain the C–V data at 77 K. Because of the low temperature, the reverse leakage current of the junction is low enough to permit measurement of capacitance. In order to check out the validity of the low temperature measurement, the same junction was measured on a modified capacitance bridge at room temperature. InP wafers which did not show any carrier freeze out showed the carrier concentrations taken at 77 and 300 K to be identical within limits of measurement error. Wafers grown by either mole fraction or S doping control showed the same behavior, indicating the ionization energy level of the carrier is very shallow. Carrier mobilities and concentrations at 77 and 300 K were measured by the Van der Pauw technique using tin contacts [14]. Mobility data measured in this laboratory are summarized in Fig. 2.

Device fabrication proceeded by thinning wafers with Br-methanol to 50–75-μm total thickness. Conventional Au-Ge/Ni contact metallizations were deposited by dc sputtering and alloyed in a hydrogen atmosphere. Individual chips were formed by the scribe and cleave technique and were ultrasonically bonded into standard low-parasitic N-34 packages.

III. Circuit Applications

A. Impedance Measurements

Devices reported in this work have been mounted in a standard N-34-style package. This package provides a capacity of 0.1 pF and a series inductance of approximately 0.1 nH. These low package parasitics are necessary to

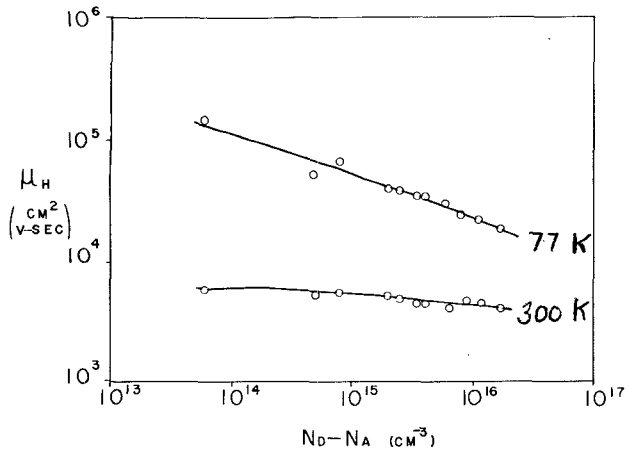

Fig. 2. Net donor concentration versus Van der Pauw hall mobility at 77 and 300 K for samples grown in this study.

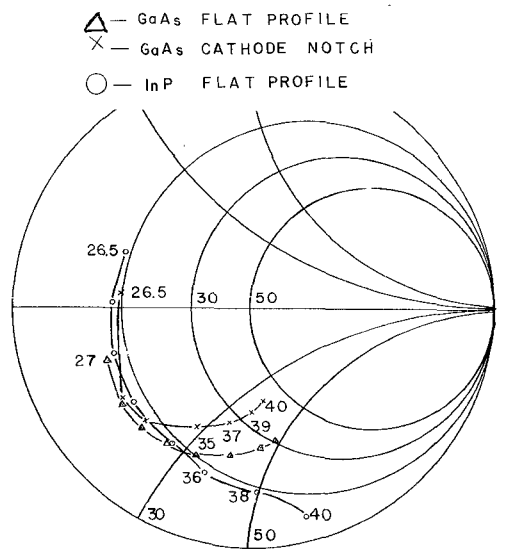

Fig. 3. Smith chart presentation of the negative of packaged device terminal impedance. Typical impedances shown are for both flat profile and cathode notch GaAs devices and for a flat profile InP device.

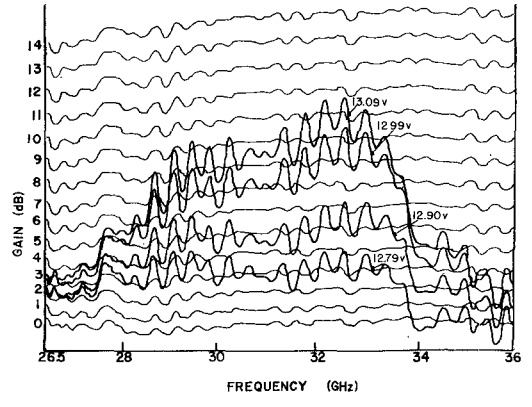

Fig. 4. Gain sensitivity of a low *Ka*-band InP amplifier to changes in bias voltage.

obtain optimum device performance in the higher frequency ranges. The ceramic dimensions for this micropill package are 0.012 in high with an outer diameter of 0.030 in [15]. The active impedance of some of these InP devices has been measured in *Ka* band using slotted-line techniques [16]. The Z matrix for a reciprocal passive two-port network thoroughly characterizes the broad-band amplifier circuits at the TEM reference plane at the end of the coaxial line center conductor. The matrix is determined by substituting three coaxial offset shorts at the diode position and calculating the circuit impedance from phase information obtained with the slotted line. The diode impedances can then be calculated from the equation

$$Z_d = Z_{12}^2/(Z_{11} - Z_{IN}) - Z_{22}$$

where Z_d is the diode terminal impedance, Z_{11}, Z_{22}, and Z_{12} are the circuit Z-matrix elements previously determined, and Z_{IN} is the measured circuit input impedance with a biased, stable negative resistance device in the circuit. With lower power high-frequency devices, care must be taken during the measurement of the device under small-signal conditions to ensure that the magnitude and phase of the reflection coefficient are not distorted by the circuit tuning effects of the moving slotted-line probe.

The negative of the terminal impedance data from typical InP Gunn devices is presented in Fig. 3. Also presented for purposes of comparison are typical impedances for flat profile and cathode notch GaAs devices optimized for *Ka*-band operation. Operating currents for the InP devices are typically 0.2–0.4 A. Other device and material parameters have been presented in earlier sections of this paper.

As can be seen from the Smith chart, the InP Gunn device negative resistance varies between 5 and 12 Ω over *Ka* band. Over the same frequency range, the GaAs devices typically exhibited negative resistances in the 13–35-Ω range. Impedance data were taken in two separate circuits optimized for the upper frequency and lower frequency portions of the band. The 26.5–34-GHz data were taken in the lower frequency circuit. The bias voltage was approximately 0.8 V higher in the lower frequency circuit. Device Q is higher for the InP devices, being typically 7.7 as compared to 4.1 for the GaAs devices evaluated, although the negative resistance does not vary as much over the same frequency range.

One other characteristic which differentiates the InP devices tested from GaAs devices is an apparent increased sensitivity of the negative resistance to changes in bias voltage. InP devices from several wafers typically exhibited an 11-percent change in negative resistance for a 0.1-V change in bias near the maximum negative resistance bias point. GaAs devices with similar profiles yielded a 3-percent change when measured in the same manner.

Fig. 4 presents a typical gain response of a lower frequency amplifier as a function of bias voltage. Shifts of the reactive portion of the device impedance appear to be more in line with those observed for GaAs devices. The figure reflects this observation in that there is virtually no frequency shift of the gain passband over the voltage range measured. The increased negative resistance sensitivity of the InP devices may reflect a nonoptimum profile for this

frequency range. It does indicate more stringent requirements on power supply noise for these devices in view of the possibly higher AM conversion in oscillator and noise figure degradation in amplifier applications.

B. InP Gunn-Effect Devices as Millimeter-Wave Oscillators

Several of our InP wafers have been evaluated in millimeter-wave oscillator circuits in the CW mode of operation. The circuit used depended upon the frequency range of interest with a coaxial circuit being used to approximately 55 GHz and a radial line circuit above that frequency. The coaxial circuit employed was similar to that described by Ruttan and Brown [17]. This circuit employs a one-half-wavelength coaxial line as the primary circuit resonator. The line is terminated at one end with the Gunn device and at the other by a coaxial low-pass filter used for bias insertion. Output coupling is accomplished by removing a portion of the coax line outer conductor near one end of the coax line. The width and height of this opening determines the coupling to the output waveguide. Some frequency tuning can be accomplished by the introduction of a dielectric rod at the high field point in the coaxial line. The coaxial line dimensions were scaled to the proper frequency range and the center conductor diameter increased slightly to provide a better match for the slightly lower negative resistance levels encountered with these InP devices as compared to GaAs devices previously evaluated. Generally, a 13-percent increase in post diameter was required to reoptimize a given circuit for best performance with the InP devices.

The radial line circuit was used for oscillators above 55 GHz because of the generally increased physical size as compared with coaxial and waveguide circuits and an apparent wider matching capability. This circuit has been described in the literature [18], [19]. Basically, the frequency of operation is determined by the diameter of the radial resonator resting on the packaged Gunn diode and the coupling by the parallel gap between the resonator and the bottom waveguide wall plus sliding short position. Other circuit elements which affect operation to varying degrees include the thickness of the radial resonator which affects output power and frequency, and the post diameter which also affects output power and, to a lesser degree, frequency. The oscillator performance measured in our laboratory is presented in Fig. 5, together with results reported by other laboratories. Results in *K* and *Ka* bands were obtained in coaxial circuits. Higher frequency results utilized radial line circuits. Some highlights of CW measurements include 200 mW and 4.6-percent efficiency at 23 GHz, 93 mW and 1.94-percent efficiency at 37 GHz, and significant power (to 78 mW) with modest efficiencies (to 1.4 percent) throughout *V* band (50–75 GHz). Device RF performance yield was very high and the power/frequency spread was low for 55-GHz devices evaluated indicating good device uniformity across the wafers. Seventy-five percent of the devices tested from one wafer in this frequency range had powers within 3 dB of the highest power and the frequencies varied by no more than 2.5 percent about the mean in the same circuit.

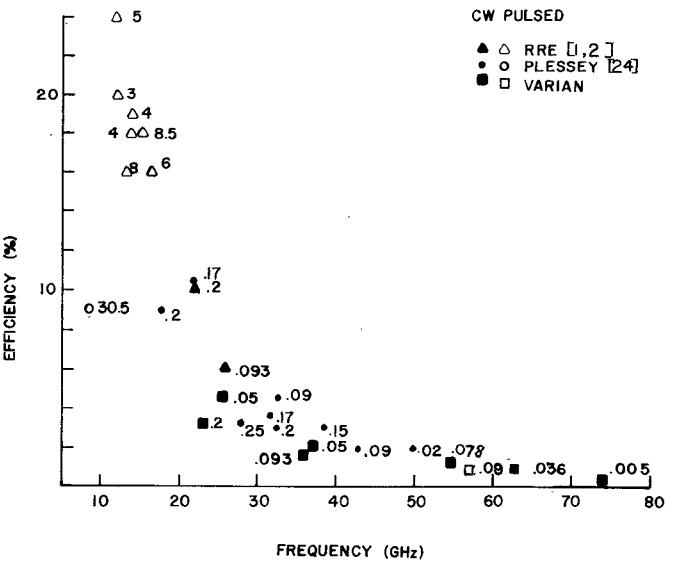

Fig. 5. Summary to date of best reported oscillator efficiencies as a function of frequency. The numbers associated with each datum correspond to output power in watts at that efficiency and frequency.

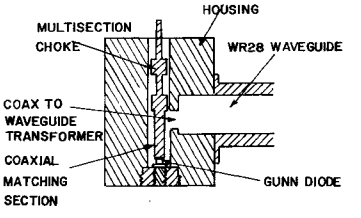

Fig. 6. Cutaway view of *Ka*-band coaxial-waveguide hybrid amplifier circuit with salient features labeled.

C. Broad-Band CW Amplifier Performance

Negative resistance diodes can be utilized for stable negative resistance amplifiers if the real part of the circuit impedance is greater than the negative resistance of the device at all frequencies where the sum of the reactances becomes zero. The matching networks must be designed to stabilize the diode and to present a reflection coefficient with constant amplitude over the desired frequency range. Several authors have presented generalized matching networks which achieve very wide bandwidth performance [20], [21]. In view of the fact that these InP devices exhibit impedance levels similar to cathode notch GaAs devices previously reported [22], similar circuit designs utilizing the coax-waveguide hybrid circuit were employed [23]. The packaged diode is imbedded at the end of a coaxial line section approximately 60° in length. A large semisection of the outer conductor is removed with the removed section facing the waveguide opening to form a broad-band coaxial-to-waveguide transition which also provides some transformation. A wide-band choke is used to terminate the opposite end of the line and to provide dc bias to the Gunn diode. A cutaway view of this circuit is shown in Fig. 6.

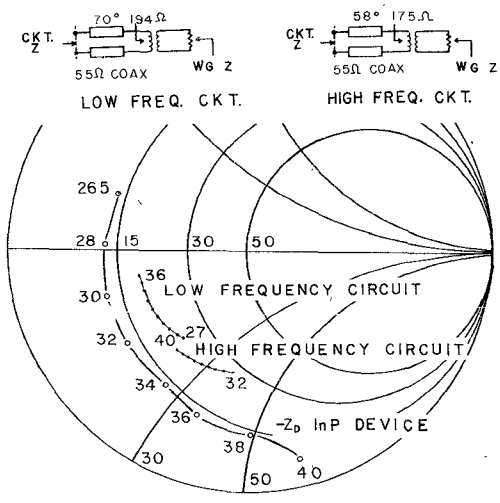

Fig. 7. Smith chart presentation of calculated circuit impedance with measured InP device impedance. Inserts show low- and high-frequency amplifier equivalent circuits.

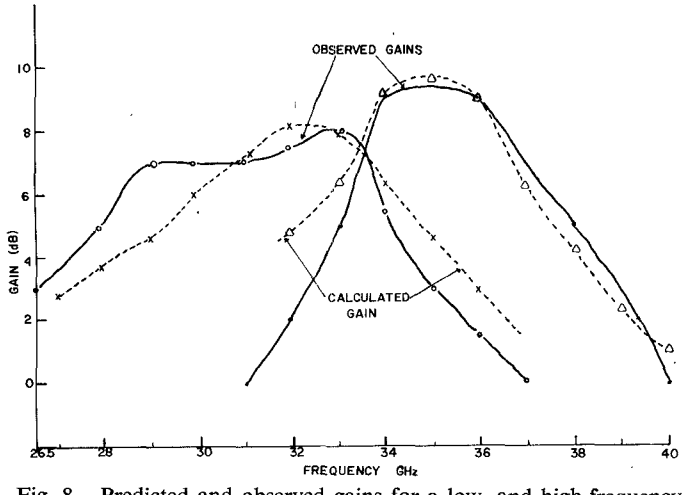

Fig. 8. Predicted and observed gains for a low- and high-frequency *Ka*-band InP Gunn-effect amplifier using the same device.

Simplified equivalent circuits for the upper and lower frequency range circuits are presented in Fig. 7. The coaxial-to-waveguide transformer is assumed to be ideal. The calculated impedances for these circuits are presented on the Smith chart. In Fig. 8 the predicted and observed gains are shown for the two half-band amplifiers using the same InP device. The lower frequency amplifier achieved 6 dB ± 0.6 dB small-signal gain over the range of 27–32.6 GHz. Bias voltage was 12.3 V and current 0.34 A. The higher frequency amplifier exhibited 9 dB ± 1 dB small-signal gain over the 34.5–38.5-GHz range. A lower bias voltage of 11.9 V was used. As shown in Fig. 8, negative resistance is available over the entire frequency band. Gain bandwidth is determined by the circuit.

Noise figures were measured at several points in the gain passband of each amplifier. Noise figures in the low-frequency circuit were in the 13–15.8-dB range with the lowest observed *Ka*-band noise figure below 33 GHz being 12.4 dB. Noise measures were generally 1–2 dB higher. High-frequency circuit noise figures were in the 14–16.5-dB range again with noise measures 1–2 dB higher. These noise figures compare very favorably with the 19–23-dB noise figures measured for GaAs devices [22] in this frequency range with similar device profiles.

Utilizing a similar but narrower band circuit scaled to the 18–26.5-GHz frequency range, a 10.1-dB noise figure has been measured with 9 dB associated gain. This represents the lowest reported InP device noise figure in this frequency range to date.

Gain compression was measured on several low-current InP Gunn-effect amplifiers operating in *Ka* band. The 1-dB compression point for these lower input power devices occurs at −10-dBm input power with an associated gain of 6 dB. Some gain expansion was observed, indicating that circuits could be further optimized for smoother compression characteristics and possibly higher saturated output powers. The devices were also measured in a 34-GHz oscillator circuit and yielded an average of 3-mW output power. Measurements indicate that oscillator output power and 1-dB compression point increase proportionally with increasing device dc input power.

IV. Conclusion

InP devices have been demonstrated to be viable two-terminal negative resistance elements for millimeter-wave applications. Significant advantages over GaAs devices including lower noise and higher frequency operation have been demonstrated. The VPE technique was used to grow thin high-quality InP layers. Progress in the material growth and evaluation areas including improved impurity level control and material evaluation methods have enabled CW operation of InP devices at millimeter-wave frequencies. The standard Au Ge/Ni contact, developed for GaAs devices, was used for ohmic contacts. Scribe and cleaved devices were hermetically sealed in low-parasitic packages, and the packaged devices have been utilized in both amplifiers in the 20–40-GHz frequency range and oscillators in the 30–70-GHz range. The millimeter-wave results reported here represent some of the highest observed oscillation frequencies for this type of device to date. Likewise, amplifier bandwidths, gains, and noise figures represent significant advancement in the state-of-the-art of millimeter-wave InP devices.

Typical InP device impedances have been measured in the 26.5–40-GHz range and compared with similarly structured GaAs devices. From this device impedance information, partial band amplifier circuits were designed and fabricated. RF evaluation of these amplifiers revealed close agreement with predicted gains and bandwidths. Noise figures measured on flat profile devices showed significant improvement over similar GaAs devices, and if the same improvements observed with GaAs devices utilizing cathode notch structures can be achieved with similar profiles in InP, reproducible noise figures of 8–10 dB in the 26.5–40-GHz frequency range appear quite feasible.

ACKNOWLEDGMENT

The authors wish to thank D. Tringali, C. Hooper, and C. Casau for their help with material growth and evaluation, and Dr. G. Antypas for the growth of InP substrate material. They also wish to thank R. Hendricks and T. Hierl for their assistance with device fabrication and evaluation.

REFERENCES

[1] K. W. Gray *et al.*, "Current limiting contacts for InP transferred electron devices," in *Proc. 5th Cornell Elect. Eng. Conf.*, pp. 215–244, 1975.
[2] D. J. Colliver, "Progress with InP transferred electron devices," in *Proc. 4th Cornell Elect. Eng. Conf.*, pp. 11–20, 1973.
[3] S. Baskaran and P. N. Robson, "Noise performance of InP reflection amplifiers in *Q*-band," *Electron. Lett.*, vol. 8, pp. 137–138, 1972.
[4] R. M. Corlett, I. Griffith, and J. J. Purcell, "Indium phosphide CW transferred electron amplifiers," *Electron Lett.*, vol. 10, pp. 307–308, 1974.
[5] J. E. Sitch, "Computer modelling of low noise indium phosphide amplifiers," *Electron. Lett.*, vol. 10, pp. 74–75, 1974.
[6] W. Fawcett and G. Hill, "Temperature dependence of the velocity/field characteristics of electrons in InP," *Electron. Lett.*, vol. 11, pp. 80–81, 1975.
[7] H. Kroemer, private communication.
[8] J. E. Sitch and P. N. Robson, "Noise measure of GaAs and InP transferred electron amplifiers," in *Proc. European Microwave Conf.*, 1974, London: Pitman Publishing, pp. 232–236.
[9] R. C. Clarke, B. D. Joyce, and W. H. E. Wilgors, "The preparation of high purity epitaxial InP," *Solid State Commun.*, vol. 8, pp. 1125–1128, 1970.
[10] B. Cairns and R. D. Fairman, "Effects of the $AsCl_3$ concentration on electrical properties and growth rates of vapor grown epitaxial GaAs," *J. Electrochem. Soc.*, vol. 115, p. 327C, 1968.
[11] ——, "Effect of the $AsCl_3$ concentration on impurity incorporation in vapor growth epitaxial GaAs," *J. Electrochem. Soc.*, vol. 117, p. 197C, 1970.
[12] R. C. Clarke, "A study of the molar fraction effect in the PCl_3–In–H_2 system," *J. Cryst. Growth*, vol. 23, pp. 166–168, 1974.
[13] M. J. Cardwell and R. F. Peart, "Measurement of carrier-concentration profiles in epitaxial indium phosphide," *Electron. Lett.*, vol. 9, pp. 88–89, 1973.
[14] L. J. Van der Pauw, "A method of measuring specific resistivity and hall effect of discs of arbitrary shape," *Philips Res. Rep.*, vol. 13, pp. 1–9, 1958.
[15] F. B. Fank and G. F. Day, "High CW power *K*-band Gunn oscillators," *Proc. IEEE* (Letter), vol. 57, pp. 339–340, 1969.
[16] J. G. de Koning *et al.*, "Gunn effect amplifiers for microwave communication systems in *X*, *Ku*, and *Ka*-bands," *IEEE Trans. Microwave Theory Tech.*, vol. MTT-23, pp. 367–374, 1975.
[17] T. G. Ruttan and R. E. Brown, "High frequency Gunn oscillators," in *Proc. Intl. Electron Devices Meeting*, Washington, DC, 1972.
[18] I. S. Groves and D. E. Lewis, "Resonant-cap structures for IMPATT diodes," *Electron Lett.*, vol. 8, pp. 98–99, 1972.
[19] T. G. Ruttan, "High frequency Gunn oscillators," *IEEE Trans. Microwave Theory Tech.*, vol. MTT-22, pp. 142–144, 1974.
[20] M. E. Hines, "Negative-resistance diode power amplification," *IEEE Trans. Electron Devices*, vol. ED-17, pp. 1–8, 1970.
[21] W. J. Getsinger, "Prototypes for use in broadbanding reflection amplifiers," *IEEE Trans. Microwave Theory Tech.*, vol. MTT-11, pp. 486–497, 1963.
[22] J. G. de Koning, R. E. Goldwasser, and S. I. Long, "Final technical report on full band transferred electron amplifiers," prepared for Naval Electronics Laboratory Center, San Diego, under contract N000123-74-C-0644, Feb. 1975.
[23] R. E. Goldwasser and F. E. Rosztoczy, "Gunn diodes for full band oscillators and amplifiers," *4th European Microwave Conf. Digest of Tech. Papers*, Montreux, Sept. 1974.
[24] The Plessey Co. Ltd, private communication.

Generation of Millimeter-Wave Signals of High Spectral Purity

ALFREDO A. CASTRO, MEMBER, IEEE, AND FRED P. ZIOLKOWSKI, MEMBER, IEEE

***Abstract*—The generation of millimeter-(mm-) wave signals phase coherent to a lower frequency reference or standard implies a large multiplication factor with inherent amplification of the short term instability or phase noise. This effect which usually is of secondary importance at lower microwave frequencies may become a limiting factor in the implementation of some mm-wave digital communication systems. Techniques used for the generation of signals of high spectral purity are discussed, and illustrated with the realization for a low data rate mm-wave satellite communications system. Quantitative results are presented and analyzed in terms of the theoretical time and frequency domain relationships.**

I. INTRODUCTION

THIS PAPER deals with the general theoretical considerations, approach, and state-of-the-art limitations for the generation of mm-wave signals of high spectral purity. It is well known that all frequency sources or generators exhibit frequency instabilities or fluctuations causing the instantaneous frequency $v(t)$ to be a random process with the addition of deterministic (hum, spurious, etc.) perturbations. As a result of these fluctuations, the ideal spectral line representing the frequency v_0 in the frequency domain will be broadened into a continuous power spectral density $S(f)$ plus the discrete lines representing the deterministic perturbations. Several terms and definitions are commonly used to characterize these frequency fluctuations such as long and short term stability, phase jitter, rms equivalent deviation, etc. Other definitions are used in the frequency domain to characterize spectral purity, such as phase and frequency noise power spectral density, sideband level with respect to the carrier, etc.

The sharpness of $S(f)$ is a graphical indication of the spectral purity of the frequency source. When this signal is angle modulated, the spectral broadening by frequency

Manuscript received February 2, 1976; revised May 10, 1976.
The authors are with the Communication Systems Laboratory, Raytheon Company, Sudbury, MA 01776.